# CHAPTER IV

# RESULTS AND DISCUSSION

This chapter was divided into five parts. The first part was the synthesis of *N*-butyl chitosan. Both *N*-butyl chitosan and chitosan were used to preparation of particles designed for controlled release of glucosamine in the second part. The particle was prepared by ionotropic gelation of the chitosan and alginate. The characterization of the particles such as size, zeta potential, morphology, and the amount of GH in the particles were investigated. Then the release profiles of glucosamine from the GH-loaded particles and carbopol containing GH-loaded particles were determined. Finally the physical stability glucosamine were reported in the last part.



## 4.1 *N*-butyl chitosan synthesis – controlling *N*-butylation on chitosan

*N*-butyl chitosan was synthesized by reductive butylation at the amino group of chitosan. Ethanol was added to improve the homogeneity of the reaction mixture because butyraldehyde was not soluble in 1% aqueous acetic acid. The amino behaves as a nucleophile attacking the carbonyl group of the aldehyde. The reducing agents were used to reduce the imine. Sodium cyanoborohydride ($NaCNBH_3$) was selected in this works because $NaCNBH_3$ was more reactive and selective than other reducing agents such as sodium borohydride ($NaBH_4$). When $NaBH_4$ was added into 1% acetic acid, it decomposed and bubble formed suddenly. In addition $NaBH_4$ works well at higher pH (~6), it is not suitable to do this for the chitosan solution because chitosan can precipitate at and above this pH. There is also a report that when using $NaCNBH_3$, reduction of aldehyde or ketone is negligible in this pH range [5].

The results of *N*-butyl chitosan synthesis are shown in Table 4.1. It should be noted that product yields were based on the assumption that one amino group reacted with only one butyraldehyde molecule.

**Table 4.1** Physical appearance and yield of *N*-butyl chitosan by controlling a proportion of butyraldehyde to amino group on chitosan

| Mole ratio CHO : $NH_2$ | Physical Appearance | %Yield |
|---|---|---|
| 0.1 : 1 | Light yellow powder | 90 |
| 0.5 : 1 | Light yellow powder | 98 |
| 1 : 1 | Light yellow powder | 84 |
| 2 : 1 | Light yellow powder | 91 |

**Table 4.2** Chemical shift ($\delta$) of *N*-butyl chitosan

| Chemical shift ($\delta$) (ppm) | Assignment | Area integration of each equivalent of butyraldehyde | | | |
|---|---|---|---|---|---|
| | | 0.1 | 0.5 | 1.0 | 2.0 |
| 0.7 | -NH-$CH_2$-$CH_2$-$CH_2$-***$\underline{CH_3}$*** | 87.3 | 90.0 | 100.0 | 100.0 |
| 1.2 | -NH-$CH_2$-$CH_2$-***$\underline{CH_2}$***-$CH_3$ | 31.8 | 34.4 | 31.0 | 58.4 |
| 1.5 | -NH-$CH_2$-***$\underline{CH_2}$***-$CH_2$-$CH_3$ | 22.5 | 22.7 | 15.6 | 44.7 |
| 3.5-4.0 | -NH-***$\underline{CH_2}$***-$CH_2$-$CH_2$-$CH_3$ | 580.2 | 166.2 | 52.5 | 40.1 |
| 3.0 | H-2 of chitosan | 111.9 | 32.1 | 16.8 | 24.0 |

4.1.1 Structure characterization

*N*-butyl chitosan

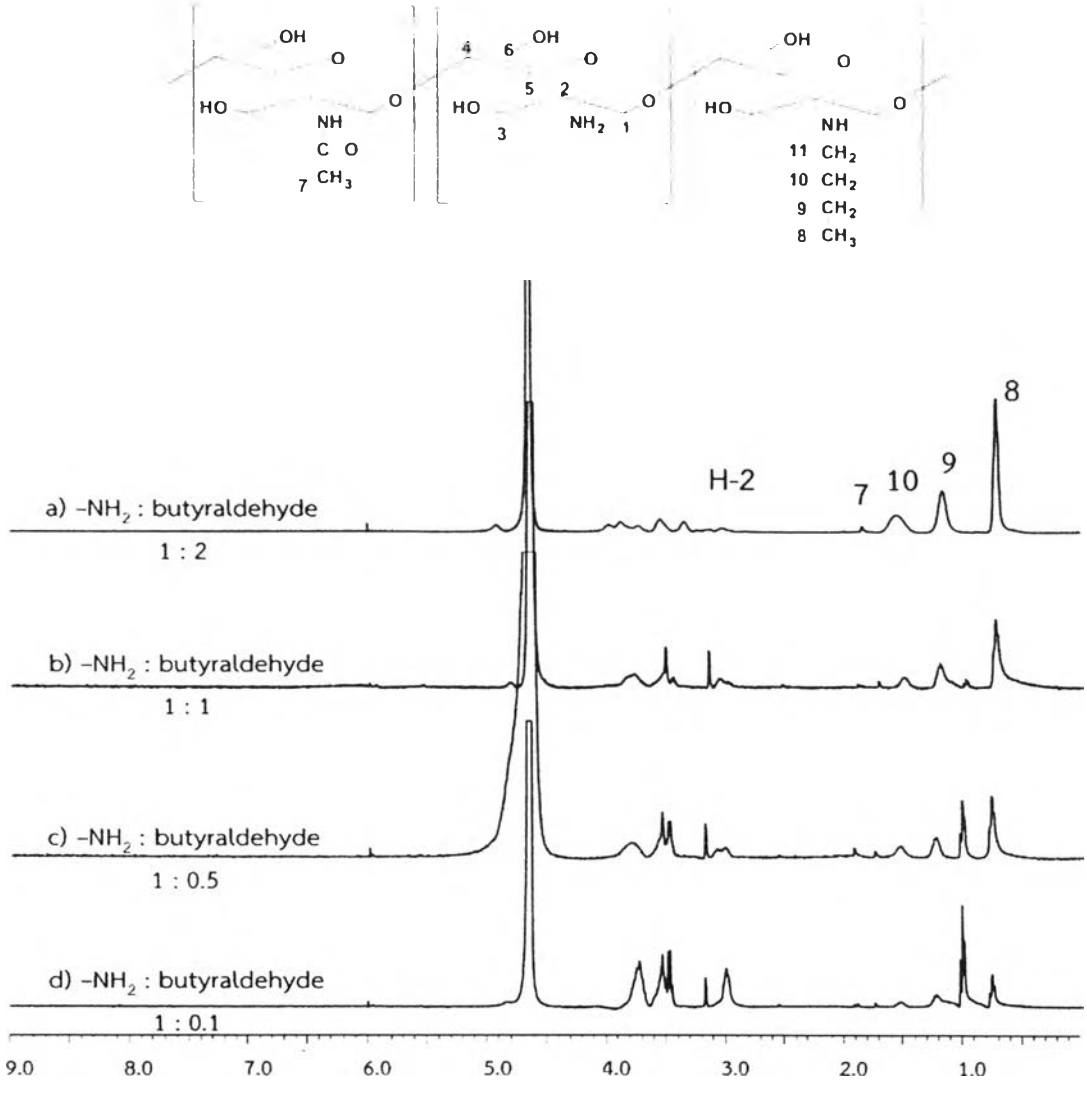


Figure 4.1 $^1$H NMR spectra of *N*-butyl chitosan

The degrees of butyl group substitution (DS) on the chitosan as a function of butyraldehyde mole equivalents were determined by $^1$H-NMR analysis (Fig 4.1, Table 4.2). The area integration of each peak was used to calculate the DS. However, the area ratio of the peak no. 8, 9, and 10 does not fit with the theoretical value of 3:2:2 for $CH_3$:$CH_2$:$CH_2$, see Table 4.2. The areas of signals no.8 ($CH_3$) and 9 ($CH_2$) are more intense than expected. This indicated one possibility that there was butyraldehyde or its reducing form (butanol) left in the product. A signal for proton at C-1 of butyl alcohol was observed in the spectrum at 3.2 ppm. Based on the information, the proton signal at peak no. 10 ($CH_2$) was used to determine degree of butylation. The degrees of butyl substitution calculated from the $^1$H-NMR analysis are shown in Table 4.3.

**Table 4.3** Degree of substitution (DS) of butyl group on chitosan

| Mole ratio of CHO:-$NH_2$ | Integration value | | %DS |
|---|---|---|---|
| | H-2 of chitosan | H-10 of butyl group | |
| 0.1:1 | 111.9 | 22.5 | 10 |
| 0.5:1 | 31.0 | 22.8 | 37 |
| 1:1 | 16.8 | 15.6 | 46 |
| 2:1 | 24.0 | 44.7 | 93 |

Increasing the butyraldehyde amount resulted in the increase of DS. At the mole ratio of 1:1, the obtained DS value was, however, only 46%, less than the expected complete substitution (100%DS). Attempts were made in order to increase the DS by increasing the aldehyde amount to two times of the amino groups present in the chitosan (mole ratio of 2:1), but it was found that the product obtained became insoluble in acetic acid solution. This was probably due to the presence of high butyl group content in the chitosan that prevented effective solvation by water molecules. The insoluble product cannot be used in the particle preparation. Therefor this works preferred to use *N*-butyl chitosan with DS that it is was not over 50% for the particle preparation.

## 4.2 Particles preparation

Glucosamine (GH) loaded calcium alginate-chitosan particles were prepared by ionic gelation method. The optimum mass ratio of sodium alginate:$CaCl_2$:chitosan to obtain the smallest particle size was 10:2.33:1, following the work reported by De and Robison in 2003 [5]. In this work, the particles were prepared by using either *N*-butyl chitosan or chitosan in the particle formulation.

The morphology of GH loaded calcium alginate-chitosan particles was analyzed by transmission electron microscopy (TEM). TEM micrographs in Fig. 4.2 reveal spherical shapes for GH-ALG-CTS and GH-ALG-46%NBC. Since the main particle compositions are cationic chitosan and anionic alginate, two staining reagents were used to investigate them; phosphotungstic acid (PTA) for positive-charge (chitosan) and uranyl acetate (UA) for negative-charge (alginate) staining. From Fig. 4.2a-b of PTA stained particles, a thin dark layer of chitosan was observed. In the UA stained particles (Fig 4.2c-d), the particle cores in both pictures are distinctively darker than outside layer, indicating that majority of core part is alginate. This result exposed a structure of particles that chitosan or *N*-butyl chitosan was coated on calcium alginate that GH was inside.

The particle size, size distribution and zeta potential were measured by Zetasizer Nano ZS (Malvern Co., UK). The characteristics of the obtained particles are shown in Table 4.4

**Table 4.4** Characteristics of GH loaded calcium-alginate-chitosan and calcium-alginate-*N*-butyl chitosan particles

| Sample | Mean size (nm) | Size dispersity | Zeta potential (mV) |
|---|---|---|---|
| GH-ALG-CTS | 294.80 ± 10.74 | 0.36 ± 0.05 | -28.50 ± 0.53 |
| GH-ALG-10%NBC | 333.37 ± 12.65 | 0.39 ± 0.06 | -29.00 ± 1.28 |
| GH-ALG-37%NBC | 364.37 ± 18.51 | 0.58 ± 0.00 | -27.57 ± 0.47 |
| GH-ALG-46%NBC | 398.30 ± 21.41 | 0.41 ± 0.09 | -26.17 ± 0.45 |

Compared with the particle from calcium alginate chitosan, the use of *N*-butyl chitosan instead of chitosan led to particle sized increase from 295 (GH-ALG-CTS) to as large as 398 nm when the amount of N-butyl chitosan in the chitosan chains reached 46%. This is most likely because the pendent butyl groups prevent closed packing of the chitosan chains. Therefore all polymer chains are farther apart, leading to the increase of particle size. The polydispersity index of particles, indicating a particle size distribution, is not over 1, suggesting that the values are acceptable for this technique. The zeta potentials of particles are ranged from -26 to -29 mv for all polymer types, showing their fair stability in colloid system.

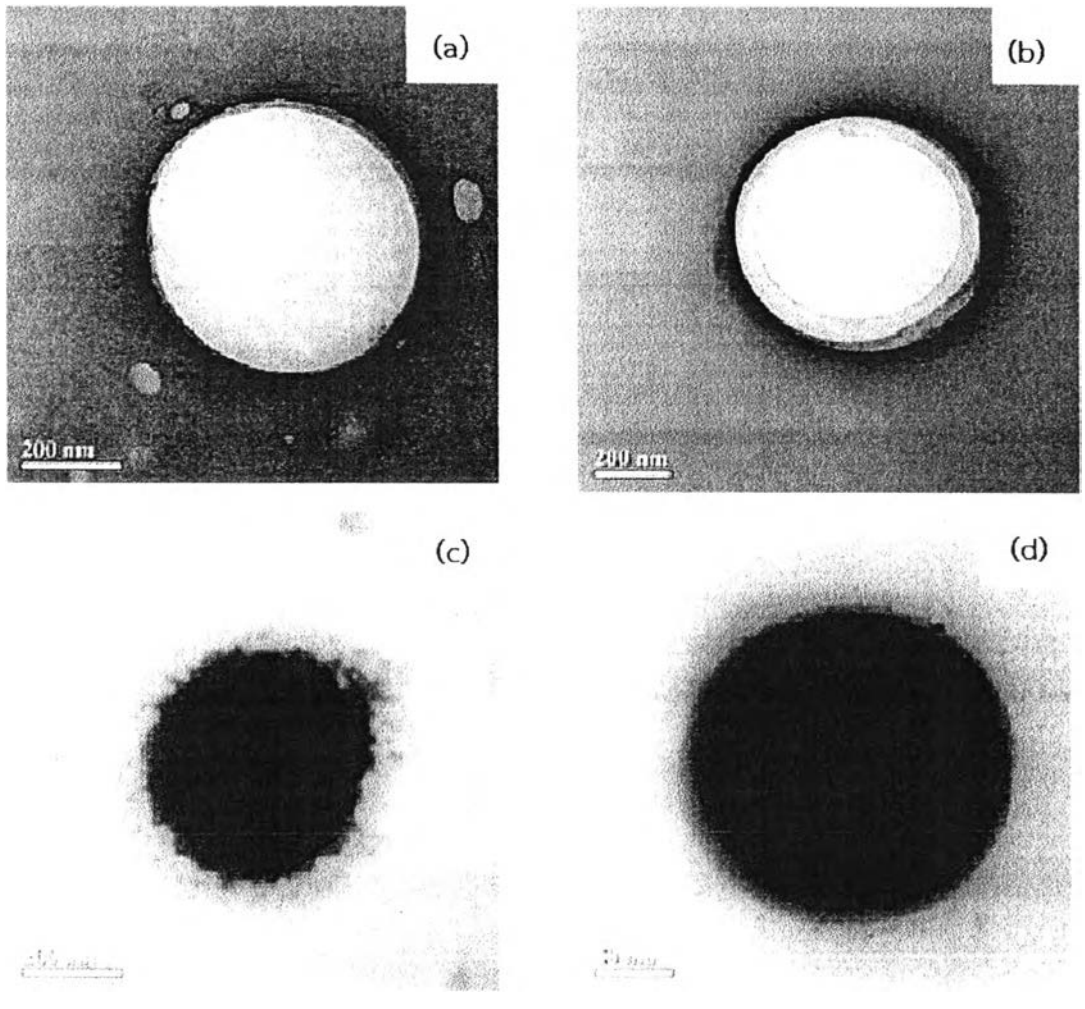


Figure 4.2 Transmission electron micrographs of particles: (a) GH-ALG-CTS and (b) GH-ALG-46%NBC stained by phosphotungstic acid; (c) GH-ALG-CTS and (d) GH-ALG-46%NBC stained by 1% uranyl acetate

The separation of particles was carried out by two methods-ultracentrifugation at 45,000 rpm and centrifugation at 5,000 rpm with membrane centrifuge tube (Amicon Ultra-15, 100K Da cut off). GH was incorporated in the particle by adding equal weight of GH and Alg (1:1 weight ratio). Both chitosan and chitosan with 46% butylation were used to prepare the GH-loaded particles. The obtained particle yields are shown in Table 4.5.

**Table 4.5** Comparison of particle yields obtained from two particle separation methods

| Sample | %Yield[1,2] from Ultracentrifuge | %Yield[1,2] from centrifugal filter tube |
|---|---|---|
| GH-ALG-CTS | 18.2 ±2.1 | 51.8 ±8.3 |
| GH-ALG-46%NBC | 17.3 ±1.8 | 58.3 ±5.2 |

[1]compared to the sum of total polymer weight and GH used in the formulation

[2]The data shown were averaged from 3 sets of experiments.

The percentage yields between the two separation methods were significantly different. The amount of particles obtained from using the centrifugal filter tube was about two times higher than the ultracentrifuge method without the filter tube. In a similar particle preparation method reported elsewhere [Aranee 2007, [24]] using ultracentrifuge (50,000 rpm) to separate chitosan-coated alginate particles resulted in 13-18% particle yield. Particles with diameter less than 100 nm remained in the suspension. The nanoparticles were not completely separated from the suspension.

Moreover it was interesting to find out whether any smaller particle remained in the filtrate after separation. An attempt to use SEM to analyze the existence of particles was not successful (Fig. 4.3). From the micrographs, only crystals of inorganic ions of $Ca^{2+}$, $Na^{-}$ were observed in both the filtrate (Fig. 4.3A) and the particle gel (Fig. 4.3B). It was possible that particles formed flat surface and could not be distinguished by SEM analysis.

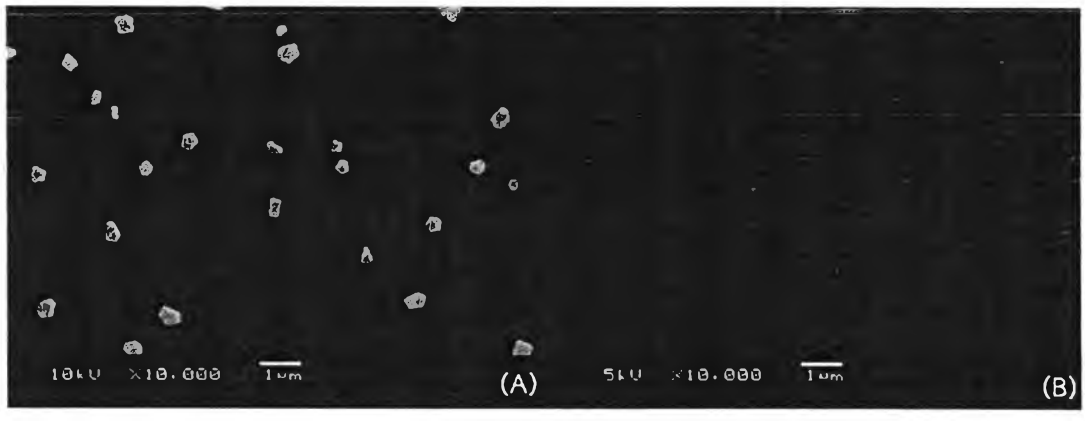


**Figure 4.3** SEM micrographs of separated components after centrifugation using centrifugal filter tube (A) filtrate and (B) filtered solid



An additional attempt to find traces of particles in the filtrate was carried out by dynamic light scattering. Particle with the average size of 100-180 nm was evidently found by the DLS analysis (see in Appendix A) while the average particle size formed in the suspension before the separation step was 295 nm. The centrifugal filter tube could not completely separate the particles that smaller than 100 nm but a membrane sort out high molecular weight particles to trap on the membrane surface.

### 4.3 Evaluation of GH contents

The content of glucosamine within the particles made of $Ca^{2+}$-alginate-chitosan and $Ca^{2+}$-alginate-NBC were analyzed by using HPLC technique. Each sample was derivatized by reacting with PITC before the analysis. The mechanism of phenylthiocarbonyl-glucosamine synthesis is shown in Fig. 4.4

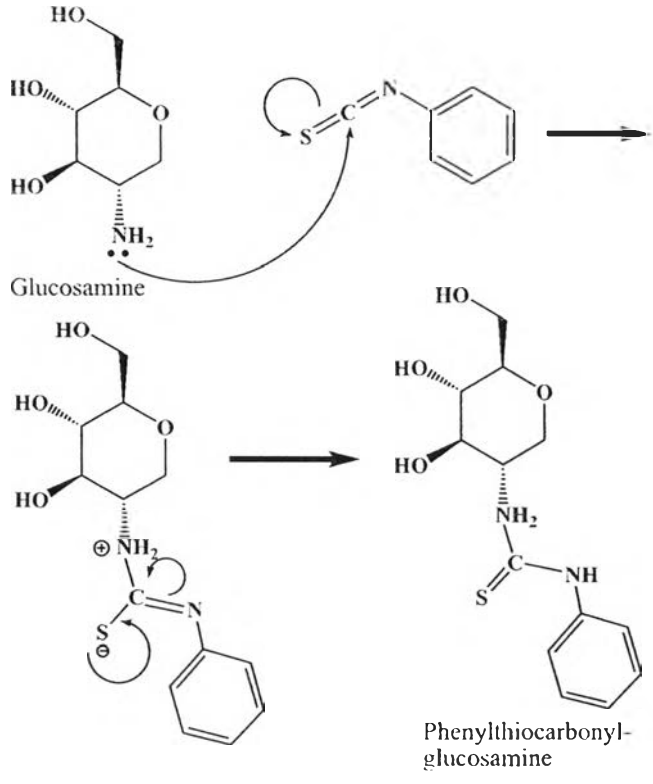


Figure 4.4 Reaction mechanism of phenylthiocarbonyl-glucosamine synthesis from glucosamine and phenylisothiocyanate

The structure of phenylthiocarbonyl-glucosamine was confirmed by $^{1}$H-NMR (Fig. 4.5). Determination of peak area ratio between glucosamine protons to aromatic protons of PITC (expected 1:1) was used to confirm the structure.

Integration of glucosamine unit = $\int(H3 - H6, H6')/5$ = 57.8/5 =11.56

Integration of aromatic unit = $\int(Aromatic\ protons)/5$ = 51.1/5 = 10.22

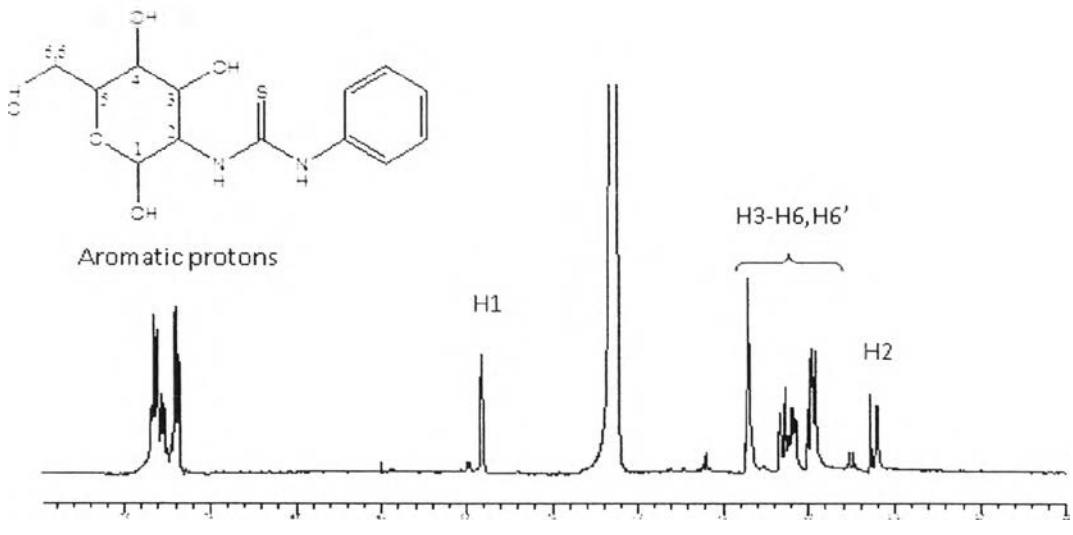


Figure 4.5 $^{1}$H NMR spectrum of phenylthiocarbonyl-glucosamine

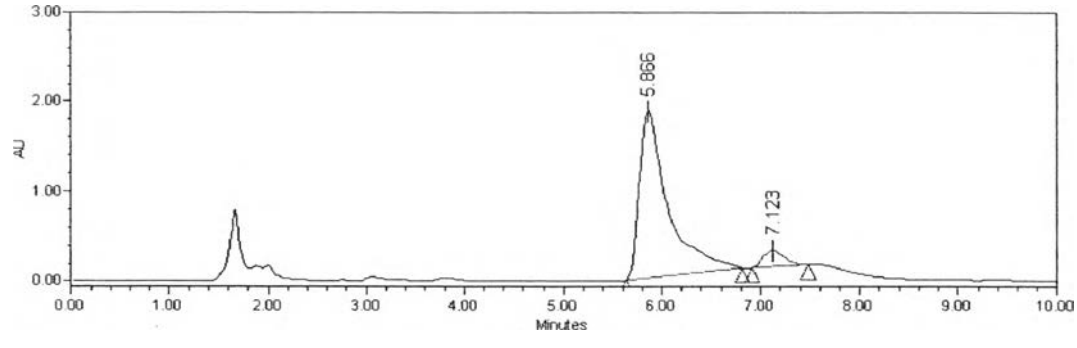


Figure 4.6 A HPLC chromatrogram of 500 µg/ml phenylthiocarbonyl-glucosamine at flow rate 1.5 ml/min with retention time 5.866

Ratio of GH:PITC was found to be 1.1:1 close to the theoretical ratio, HPLC chromatogram of phenylthiocarbonyl-glucosamine is shown in Fig. 4.6. Retention time of the GH-derivative was 5.866 and peak at 7.123 which was anomeric form of glucosamine.

The GH loading efficiency (LE) was calculated as the percentage of GH loaded in particles compared with the initial amount of GH added in the formulation and GH loading capacity (LC) was calculated as the percentage of GH loaded in particles compared with total weight of dried GH-loaded particles. After the particles were separated from the suspension by centrifugal filter tube, they were broken down by

addition of sodium citrate solution. Since sodium citrate is smaller than alginate polymer, sodium citrate can replaced the alginate also by ionic interaction between its carboxylate group and the amino group of chitosan causing particle rupture.

Because separation of particles by centrifugation cannot completely separate liquid medium from the particles, the free GH may collect on the surface of the particles, leading to higher LE than expected. The GH loaded content in particles could be calculated by estimating the amount of GH in the obtained particles and the free GH recovered from the filtrate after centrifugation. The LE values of GH which have a different GH:ALG mass ratio are shown in Table 4.6.

From the LE results, it seems that having NBC in the formulation helped increase the LE of GH in the particles. It was, however, found that the LE was not depending on the GH to polymer weight ratios from 1:1 to 5:1.The ratio of GH:ALG of 2.5:1 was chosen in all experiments in the coming sections because the GH content was high enough to be clearly detected by the chosen analysis means.

Table 4.6 The influence of GH:ALG mass ratio on loading efficiency of different types of GH-loaded particles

| Type of Particles / mass ratio GH:ALG:CTS | % Loading efficiency | | |
|---|---|---|---|
| | 1:1:0.05 | 2.5:1:0.05 | 5:1:0.05 |
| GH-ALG-CTS | 53 ± 1 | 50 ± 2 | 61 ± 1 |
| GH-ALG-10%NBC | 55± 2 | 56 ± 3 | 55 ± 2 |
| GH-ALG-37%NBC | 61 ± 1 | 60 ± 8 | 62 ± 5 |
| GH-ALG-46%NBC | 60 ± 1 | 66 ± 2 | 64 ± 1 |

All data shown were averaged from three sets of experiments

Dried GH-loaded particles were immersed in sodium citrate solution in order to recover all GH trapped in the particles. The results of LE and LC of different types of GH-loaded particles are displayed in Table 4.7. Comparing among the particles having three different NBC contents (10, 37, and 46%NBC), LE and LC was increased when the butyl content in the particles increased. However the net amount of

loaded GH in the particle was low. It was possible that GH was easily dissolved in water. It tended to release out from the particles very fast during every step of particle preparation as well as during storage.

Application of GH-loaded particles was planned to use in formulation of gel. Each batch of particle preparation, the hydrated particles were collected and total used in gel formula. Therefore LE was indirectly calculated by determining GH content in filtrate. Another observation will be made here that the sum of GH amount in the particle and filtrate was lower than 100. It was possible that some GH or particles stuck to centrifuged tube or lost during sample transfer.

GH Loading efficiency values (LE) were 42% in GH-ALG-CTS, 36% in GH-ALG-10%NBC, 52% in GH-ALG-37%NBC, and 67% in GH-ALG-46%NBC (Table 4.8). It should be noted that the GH recovery was not 100%. This was probably caused by rapid release of GH from the particles. The results in 4.4.1 showed that GH was quickly released from the particles in three hours. Since the procedure to prepare the particles for LE determination, from preparation of suspension until particle separation, required a long time (~24 h). Although, the samples were kept in a refrigerator (5°C) to retard the release of GH but it still released out of the particles. If this is the case, the LE values shown in Table 4.8 cannot be determined correctly.



**Table 4.7** The GH content, the loading efficiency of GH and the loading capacity of GH in the particles were determined by method I (GH:alginate weight ratio of 2.5:1), all data shown were averaged from three sets of experiments

| Sample | Amount of GH in dried particles (mg) | %LE of GH[1] | %LC of GH[2] |
|---|---|---|---|
| GH-ALG-CTS | 3.0 ± 0.12 | 7.2 ± 0.3 | 44 ± 3 |
| GH-ALG-10%NBC | 2.2 ± 0.06 | 5.2 ± 0.1 | 29 ± 3 |
| GH-ALG-37%NBC | 3.0 ± 0.12 | 7.3 ± 0.3 | 41 ± 1 |
| GH-ALG-46%NBC | 4.0 ± 0.15 | 9.6 ± 0.4 | 62 ± 3 |

[1]Loading efficiency was calculated from equation (2)

[2]Loading capacity was calculated from equation (3)

**Table 4.8** The GH content, the loading efficiency of GH in particles was determined by method II and %recovery of GH (GH:alginate weight ratio of 2.5:1). All data shown were averaged from three sets of experiments

| Sample | Amount of GH in filtrate (mg) | Amount of GH in particles (mg) | %LE of GH[1] | %recovery[2] |
|---|---|---|---|---|
| GH-ALG-CTS | 24.2 ± 0.4 | 17.8 ± 0.4 | 42 ± 3 | 50 ± 0.8 |
| GH-ALG-10%NBC | 26.9 ± 1.1 | 15.1 ± 1.1 | 36 ± 3 | 41 ± 2.7 |
| GH-ALG-37%NBC | 19.9 ± 1.0 | 22.1 ± 1.0 | 52 ± 2 | 60 ± 2.1 |
| GH-ALG-46%NBC | 13.9 ± 0.8 | 28.1 ± 0.8 | 67 ± 1 | 77 ± 1.6 |

[1]Loading efficiency was calculated from equation (4)

[1]Recovery of GH was calculated from equation (5)



## 4.4 Release study

### 4.4.1 GH release study of particles in phosphate buffer medium

The GH contents in four particle types are shown in Table 4.9. These particles were subjected to release study as described in Section 3.2.4

**Table 4.9** Initial amount of GH in 5 g of particles

| Sample | Amount of GH in 5 g of particle[1] (mg) |
|---|---|
| GH-ALG-CTS | 6.7 |
| GH-ALG-10%NBC | 6.3 |
| GH-ALG-37%NBC | 8.0 |
| GH-ALG-46%NBC | 10.2 |

[1]Amount of GH determined by method II

The cumulative drug release profiles from the particles having different butyl contents of chitosan were plotted as a function of time. Release profiles of GH from four particle types are shown in Fig. 4.7. The amount of GH was quickly released in the first hour period after that the release rate was slowly decreased until equilibrium (no release) after 6 h of incubation in PBS 7.4. The cause of fast GH release was possibly due to free GH on the particle surface.

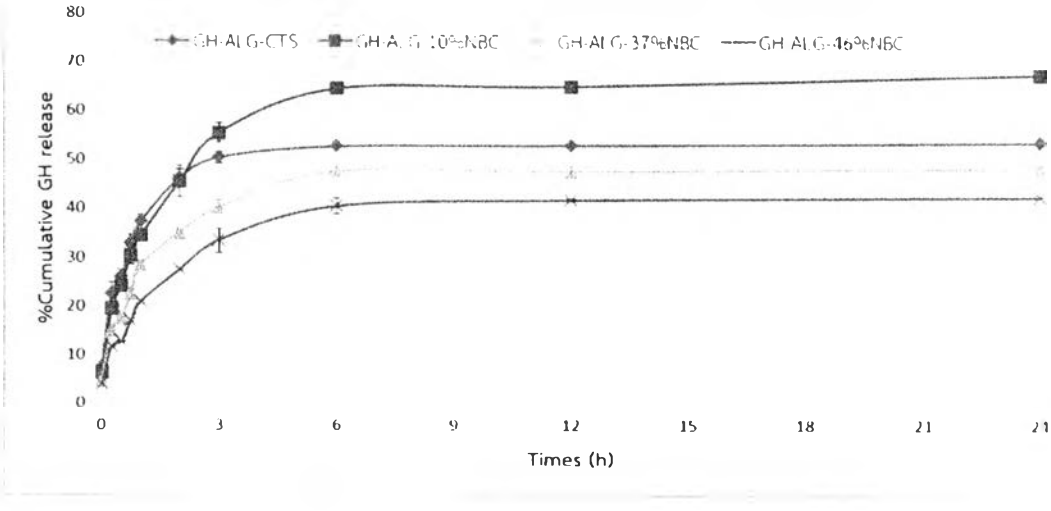


**Figure 4.7** Comparison of cumulative GH release percentage from the particles having different butyl content of chitosan (GH: alginate weight ratio =2.5: 1)

Considering the first 3 hours of release, GH was released in range of 34-56% from all particles. From Table 4.9, initial amount of GH in particles was not much different, so the effect of %butylation on release rate could be described by cumulative release profiles. The particles with low butyl content tended to GH more release and faster than the particles with high butyl content. The maximum release amounts were 67, 48 and 42% for GH-ALG-10%NBC, 37%NBC and 46%NBC particles, respectively, during the test period of 24 h (Fig. 4.7). It means that GH remained in the particle, possibly by the hydrogen bonding between the hydroxyl and amino groups of GH and those in chitosan as well as in alginate. The overall release profile of GH-ALG-CTS particles was unexpectedly lower than the GH-ALG-10%NBC particles, but its release rate in the first hour was much higher (30%) than from the latter (25%). This result proves that the hydrophobicity effect of *N*-butyl chitosan delays

the release of GH from particles although it occurs in a short period because GH is highly soluble in water.

### 4.4.2 In vitro drug permeation through membrane

In order to investigate the use of the calcium alginate chitosan particles with hydrophobic part as a controlled release system for transdermal drug delivery, the percutaneous permeation of glucosamine hydrochloride as a model drug was evaluated in the form of carbopol gel containing GH-loaded calcium alginate chitosan particles and GH-loaded calcium alginate *N*-butyl chitosan particles, using 46%DS of NBC in this study because of highest LE (67%) among other NBC.

#### 4.4.2.1 Preparation of carbopol gel containing GH-loaded particles

Many commercial products of glucosamine are available in gel-dosage form because gel product is water washable and is comfortable use in patients. Gel containing GH-loaded particle was prepared using carbopol as a gel forming and triethanolamine as a thickening agent and neutralizer. The physical properties of GH-particles carbopol gel are shown in Table 4.10.

**Table 4.10** Appearance and pH of gel preparation

| Formula | Appearance | pH |
|---|---|---|
| 1% GH-gel | Transparent gel | 7.21 |
| GH-ALG-CTS gel | Transparent gel | 7.08 |
| GH-ALG-46%NBC gel | Transparent gel | 7.15 |

#### 4.4.2.2 GH permeation profiles

The permeation of GH through the cellulose acetate membrane from 1% GH-gel, GH-ALG-CTS gel, and GH-ALG-46%NBC gel was performed by Franz-diffusion cell. After the sample was collected at each sampling time point for a total 24 h, the amount of permeated GH was calculated in terms of mean cumulative amount of permeated GH through a unit area of membrane ($Q_c$). In each sample, the $Q_c$

increased with time, indicating that GH was continuously released from the gel and permeated through the membrane to accumulate in PBS (Fig. 4.8). The permeated behaviors of GH release from all dosage gels were found to be a linear relationship with time in the first 8 hours of incubation.

The relationship between time and amount of GH permeating across membrane as well as flux values are shown in Tables 4.11. From the table, higher drug content in gel led to higher permeating flux. The GH-ALG-46%NBC gel had a slightly lower flux than the GH-ALG-CTS gel because the hydrophobicity of NBC retained GH release from the particles.

In all gel formulations, GH can release only 30-35% of the loading content after 48 h (Figure 4.9). The role of carbopol gel was also slowing down the diffusion of GH out of the gel as compared to the release study of particles discussed in Section 4.4.



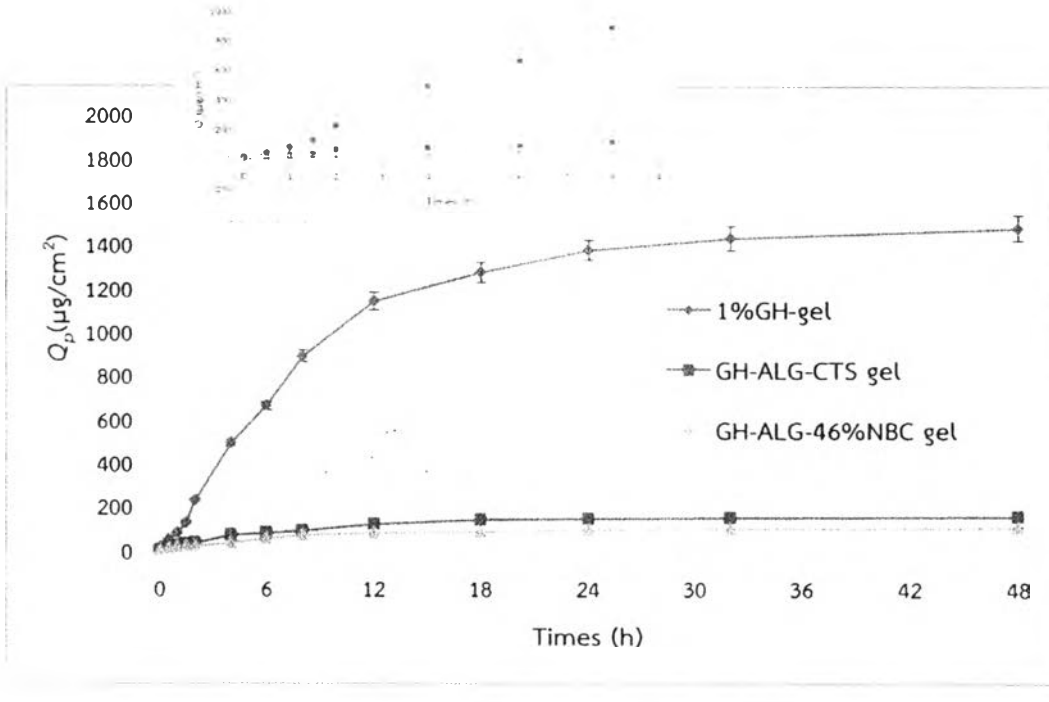


**Figure 4.8** Permeation profiles of 1%GH-gel, GH-ALG-CTS gel and GH-ALG-46%NBC gel across cellulose acetate membrane, a magnified plot of the first 8 h of incubation is also shown

**Table 4.11** Linear relationship and Flux of GH-gel, GH-ALG-CTS gel and GH-ALG-46%NBC gel across cellulose acetate membrane at 0-8 h

| Formula | Linear relationship | $R^2$ | F (μg/cm$^2$·h) |
|---|---|---|---|
| **1% GH-gel** (1.38 mg GH in 1g of sample) | $Q_t$ = 113.7t + 6.67 | 0.9934 | 113.7 |
| **GH-ALG-CTS gel** (0.44 mg GH in 1g of sample) | $Q_t$ = 12.8t + 23.07 | 0.9143 | 12.8 |
| **GH-ALG-46%NBC gel** (0.57 mg GH in 1g of sample) | $Q_t$ = 8.2t + 5.30 | 0.9848 | 8.2 |

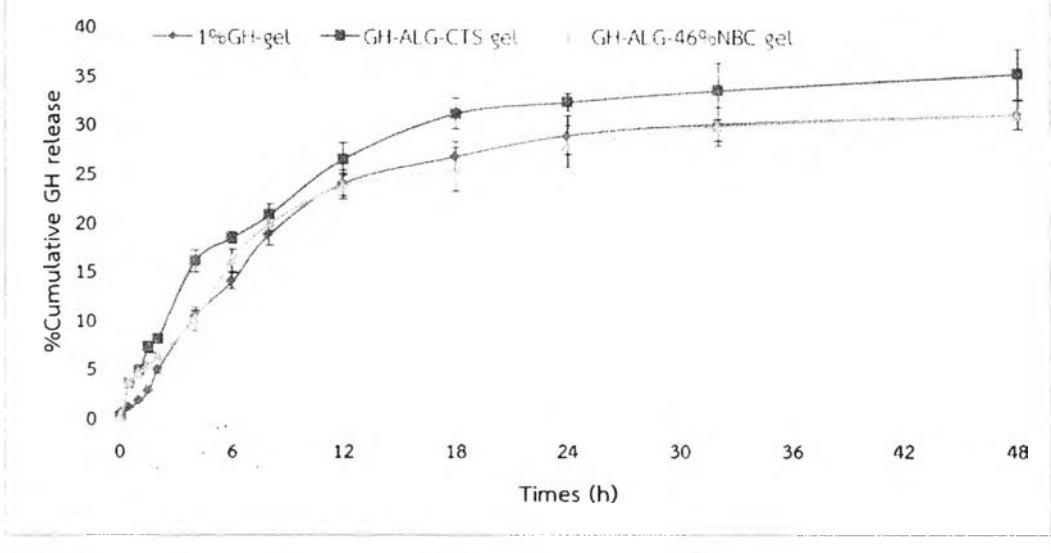


**Figure 4.9** Comparison of %cumulative GH release of 1% GH-gel, GH-ALG-CTS gel and GH-ALG-46%NBC gel across cellulose acetate membrane

## 4.5 Stability test

### 4.5.1 Physical stability in suspension of GH-loaded particles

The prepared GH-ALG-CTS particles and GH-ALG-46%NBC particles were stored at room temperature for 60 days. Physical stability of particles in suspension was checked for pH, mean particle size, and zeta potential. The results are shown in

Table 4.12. Both particles showed good stability at 7 days, with no change in pH, mean size, and zeta potential. After 15 days of storage, the pH of suspension was decreased and particle size seemed not different until 45 days but the zeta potential of particles was largely decreased. This situation indicated that particles were not stable in aqueous solution. The repulsive force of charge of particle was decreased so the particles had a chance to aggregate. It shows clearly at 60 days, the particles size of GH-ALG-CTS particles and GH-ALG-46%NBC particles was increased to 488 nm and 696 nm respectively. Therefore, the storage of particles in suspension form should not be over 7 days.

**Table 4.12** The pH, mean particle size, and zeta potential of GH-ALG-CTS particles and GH-ALG-46%NBC particles in suspension for stability tests for 60 days

| parameters | Storage periods (days) | | | | |
|---|---|---|---|---|---|
| | 0 | 7 | 15 | 45 | 60 |
| *pH* | | | | | |
| GH-ALG-CTS | 5.31 | 5.28 | 4.56 | 4.07 | 4.11 |
| GH-ALG-46%NBC | 5.44 | 5.33 | 4.68 | 4.79 | 4.66 |
| *Mean size (nm)* | | | | | |
| GH-ALG-CTS | 398 ± 6 | 376 ± 4 | 361 ± 4 | 353 ± 12 | 488 ± 6 |
| GH-ALG-46%NBC | 593 ± 11 | 585 ± 13 | 571 ± 11 | 543 ± 3 | 696 ± 3 |
| *Zeta potential (mV)* | | | | | |
| GH-ALG-CTS | -28 ± 1 | -30 ± 1 | -13 ± 0 | -12 ± 2 | -13 ±1 |
| GH-ALG-46%NBC | -29 ± 2 | -30 ± 1 | -19 ± 0 | -14 ± 3 | -9 ± 1 |

### 4.5.2 Physical stability of formula gel

Storage stability test of carbopol gel containing GH, GH-ALG-CTS particles and GH-ALG-46%NBC particles was investigated by observing with naked eyes after preparation and at 30 days for any change in the physical appearance (color and pH). The GH content in gel was evaluated by HPLC technique after fresh preparation at first day an after $30^{th}$ day.

After preparation of gel formulations, all types have a similar appearance, colorless and transparent. The small changes in pH and GH content in particles for 30 days but a change in color was observed from colorless to be brown or yellow (Fig. 4.10 and Table 4.13). The 1%GH-gel showed a brown color because it had a most content of GH; the oxidation of GH was occurred during storage.

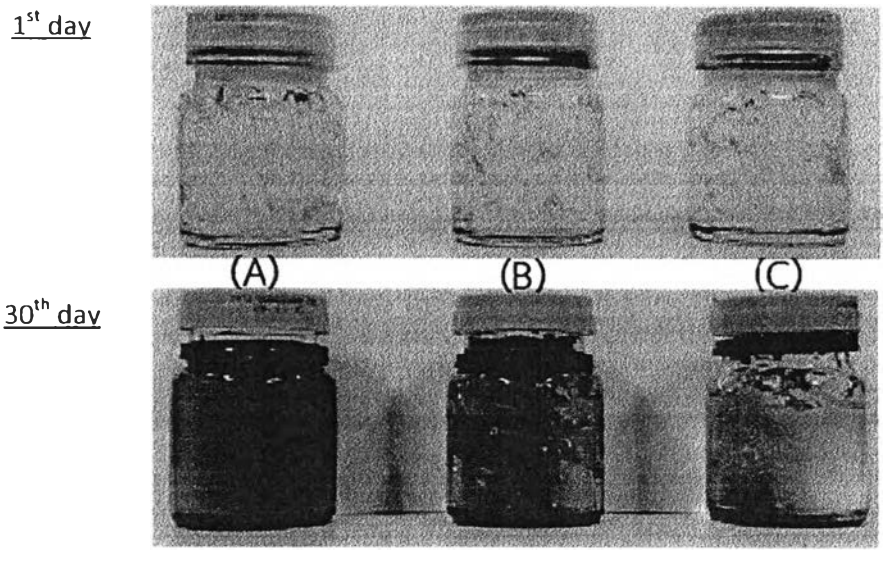


**Figure 4.10** Photographs of gel formulation stored at 1st day and 30th day; A) 1%GH-gel, B) GH-ALG-CTS gel and C) GH-ALG-46%NBC

**Table 4.13** The physical appearance and GH content of gel formulation stored at 1st day and 30th day

| Formulation | Color | | pH | | GH content (mg/g of gel) | |
|---|---|---|---|---|---|---|
| | 1st day | 30th day | 1st day | 30th day | 1st day | 30th day |
| 1% GH-gel | Colorless | Brown | 7.21 | 6.35 | 10.00 | 7.74 |
| GH-ALG-CTS gel | Colorless | Yellow | 7.08 | 6.46 | 0.44 | 0.37 |
| GH-ALG-46%NBC gel | Colorless | Light yellow | 7.15 | 6.62 | 0.57 | 0.44 |